J Mater Sci (2012) 47:2915–2927
DOI 10.1007/s10853-011-6124-1

The effectiveness of coincidence site lattice criteria in predicting creep cavitation resistance

F. Otto · E. J. Payton · J. Frenzel · G. Eggeler

Received: 16 August 2011 / Accepted: 10 November 2011 / Published online: 24 November 2011

Abstract The coincidence site lattice (CSL) concept is often used in microstructural characterization by researchers studying grain boundary engineering as a method for improving the performance of polycrystalline materials. It is assumed that a high degree of shared lattice sites in the boundary between two grains will result in improved mechanical properties. For practical application of the CSL concept to experimental results, a maximum deviation from ideal CSL orientation relationships must be defined to distinguish potential CSL boundaries from random boundaries that are not likely to exhibit "special" properties. Several different maximum deviation criteria have been proposed in the literature. In this study, four of these criteria are investigated for their effectiveness in predicting the creep cavitation resistance of boundaries of different CSL character in three model alloys: pure Cu, Cu-Bi, and Cu-Sb. Bi and Sb strongly segregate to Cu grain boundaries and are detrimental to creep life. The experimental observations are compared to simulation results for a non-textured polycrystal. It is observed that only boundaries related to cubic annealing twins ($\Sigma 3$ and $\Sigma 9$) exhibit special resistance to creep cavitation, that boundaries with $\Sigma > 3$ are affected by the presence of segregants, and that the fraction of non-$\Sigma(3,9)$ boundaries tracks closely with what would be expected from a random polycrystal. It is shown that more restrictive criteria result in more reliable characterization of the fraction of cavitation-resistant boundaries only because they exclude more non-$\Sigma(3,9)$ boundaries from the analysis.

F. Otto · E. J. Payton · J. Frenzel · G. Eggeler
Institut fuer Werkstoffe, Ruhr-Universitaet Bochum,
44780 Bochum, Germany

Present Address:
F. Otto (✉)
Materials Science and Technology Division, Oak Ridge National Laboratory, One Bethel Valley Road, Oak Ridge,
TN 37831-6115, USA
e-mail: frederik.otto@rub.de

Present Address:
E. J. Payton
Division 5.1: Composition and Microstructure of Engineering Materials, Federal Institute for Materials Research and Testing,
Unter den Eichen 87, 12205 Berlin, Germany

Introduction

Most structural engineering materials have a polycrystalline microstructure where individual crystallites are separated by grain boundaries. Although the density of grain boundaries is often deliberately increased to exploit their strengthening effect on the material (e.g., the well-known Hall–Petch relationship) [1], grain boundary related processes can also limit the service life of polycrystalline components. Examples of such damage processes are intercrystalline stress corrosion cracking [2], liquid metal embrittlement [3], and creep cavitation [4]. Among other factors, the crystallographic grain boundary character has been identified to play a major role in determining whether a grain boundary is susceptible to the occurrence of such intergranular damage processes [5–7]. Beneficial properties have been observed in grain boundaries that exhibit a high structural periodicity, such as low-Σ coincidence site lattice (CSL) boundaries [5–7]; however, mixed and inconclusive results have often been obtained for CSL boundaries that are not the product of twinning [8].

The CSL concept provides a geometric framework for describing the orientation relationships between grains by characterizing the periodicity of the coincident atomic sites

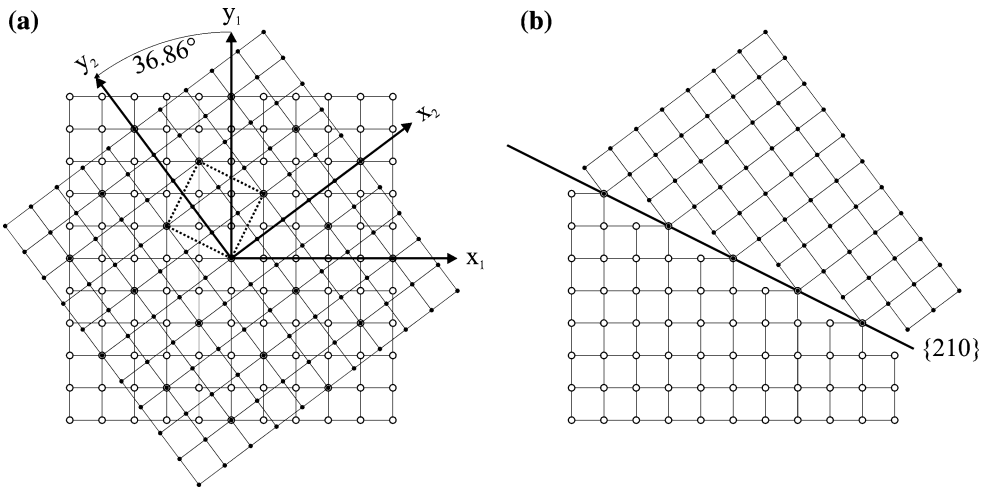

Fig. 1 **a** Top view along the [001] direction on two interpenetrating cubic lattices misoriented by 36.86°, which form a superlattice of coincident sites (*dotted rectangle*); **b** atoms lying on the {210} plane of the misoriented lattices belong to both of the adjacent crystals

of a superlattice between the lattices of the individual crystallites [8, 9]. The volume ratio of the superlattice cell and the crystal lattice cell constitutes the so-called Σ value [8], which always is a positive, odd integer. Figure 1a illustrates the CSL concept through a top view of two interpenetrating cubic crystal lattices denoted as 1 (open circles) and 2 (filled circles), which are rotated 36.86° relative to one another along their common [001] direction. The superimposed sites constituting one CSL cell are highlighted by a dotted rectangle. If the boundary plane in Fig. 1a is of the type {210} with respect to both lattices, the grain boundary exhibits a structural periodicity with atoms belonging to both grains as marked by the solid line in Fig. 1b, and the boundary is denoted Σ5. A lower Σ value corresponds to a greater percentage of atomic sites shared between the two misoriented crystal lattices, and presumably a lower interfacial energy and an improvement in mechanical properties.

Watanabe [10] suggested in his classical grain boundary design approach that beneficial properties of low-Σ CSL boundaries, in particular twin boundaries (which are Σ3 in FCC), can be exploited by increasing their number fraction in the microstructure. This has been successfully demonstrated in experimental studies on polycrystals, e.g., [11, 12]. It has been discussed up to which Σ value special properties can be anticipated and a value of 29 is often taken as a cut-off [8]. Even in the case that there exist higher-Σ CSL boundaries with special properties, they would generally appear in very small numbers [8]. A major practical problem in these studies remains the classification of CSL boundaries that truly exhibit special properties. The special properties should be lost at some point as the boundary deviates from the ideal orientation relationship because the structural periodicity will cease to exist. To assign a maximum allowed angular deviation, $\Delta\Theta_{max}$, various researchers [13–16] have proposed criteria of the form

$$\Delta\Theta_{max} = \Theta_0 \cdot \Sigma^{-n} \quad (1)$$

where Θ_0 and n are constants. Some values for these constants are given in Table 1. The resulting values for $\Delta\Theta_{max}$ for CSL boundaries with $1 \leq \Sigma \leq 29$ are shown in Fig. 2. A Σ1 boundary corresponds to a low-angle grain boundary. Although, all criteria are based upon the Read-Shockley model [17], they yield substantially different values. While the Ishida-McLean (I-M) criterion [16] is most restrictive, deviations as high as 8.66° are allowed for

Table 1 Θ_0 and n values proposed for use in Eq. 1 by various researchers

Criterion	Θ_0	n	Ref.
Brandon	15	1/2	[13]
Pumphrey	15	2/3	[14]
Palumbo-Aust	15	5/6	[15]
Ishida-McLean	8	1	[16]

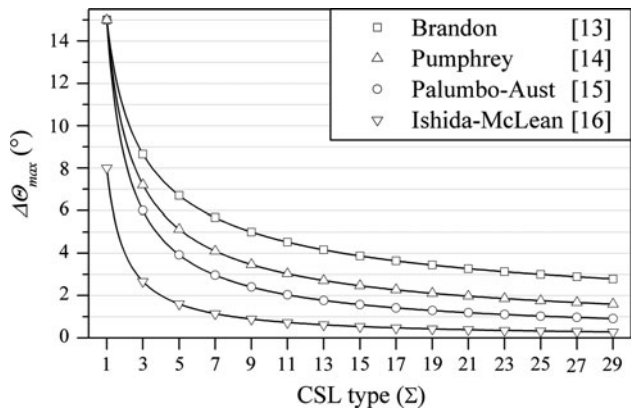

Fig. 2 Maximum allowed angular deviations from the ideal CSL orientation relationship under the criteria proposed by various researchers

the Σ3 orientation relationship according to the Brandon (B) criterion [13].

A fundamental weakness in CSL theory is that it is strictly geometric and ignores the effects of local atomic rearrangements at the interface. Nevertheless, use of CSL theory remains common in materials science because it presents a useful framework for classification of boundaries when the analysis technique does not allow for determination of the boundary plane or detailed characterization of the atomic-scale structure. Since it is questionable whether the rather rigid assumptions about lattice coincidence reflect reality in sufficient accuracy to effectively predict grain boundary properties, it is unclear the extent to which physical significance can be attributed to boundaries matching CSL criteria. Correlations between properties and the percentage of CSL boundaries can only be successful if the intrinsic properties of the boundary are closely related to the geometrical aspects of the orientation relationship between adjacent grains. The grain boundary energy, for example, changes as a function of the inclination of the boundary plane [18], and local rearrangements producing atomic-scale steps and facets aligned in energetically favorable orientations have been directly observed in studies of interfaces [19]. The CSL theory as it is generally applied (via Eq. 1) only takes into account the orientation relationship aspect, and ignores the inclination of the grain boundary plane, thus acknowledging only three of the five degrees of freedom of the grain boundary. A rotation of the grain boundary plane in Fig. 1b about a small angle would effectively destroy the short wavelength of the structural periodicity while still maintaining the orientation relationship defined in Fig. 1a. The determination of all macroscopic degrees of freedom that constitute the grain boundary structure requires techniques that allow for three-dimensional characterization of material volumes. While electron backscatter diffraction (EBSD) is not unambiguously capable of resolving this issue due to the lack of information from below the specimen surface, it allows for a high-throughput investigation of a great number of grain boundaries, and is therefore particularly useful in obtaining statistically significant results. Despite the shortcomings of the CSL concept, correlations between the percentage of boundaries having CSL character ($3 \leq \Sigma \leq 29$) and the mechanical properties have been reported to exist (e.g., [11]). Open questions remain regarding the reliability of CSL theory in the identification of boundaries that actually exhibit special properties. Furthermore, under the assumption that the percentage of CSL boundaries might serve as an indicator of special grain boundary properties, the question of which values (in Eq. 1) would be most appropriate to use reliable detection of CSL boundaries by EBSD remains open from both the practical and scientific perspectives.

The formation of creep cavities on grain boundaries under high temperature–low stress conditions is known to depend on a variety of factors, among them the crystallographic character of a grain boundary [4]. Earlier research on pure Cu under such testing conditions showed that creep cavitation is strongly heterogeneous with respect to the grain boundary character [7] and that Σ3 boundaries are particularly resistant to cavitation. The exact nature of this dependency is still unknown. One contributing influence could be the inhomogeneous segregation of residual impurities to grain boundaries [7]. In this study, we therefore investigate the influence of interfacial chemistry on the capability of four different CSL criteria to predict "specialness" in terms of cavitation resistance through Cu samples containing small amounts of Bi or Sb. The availability of statistically meaningful data on creep cavitation in pure Cu with a special focus on grain boundary crystallography [7] provides an excellent basis for comparison with our materials, which contain segregating impurities. Both Bi and Sb are known to segregate to grain boundaries in Cu [20, 21] and to facilitate cavity nucleation under creep conditions [22, 23].

Materials and methods

For this study, six model materials were produced via an ingot metallurgy processing route. In addition to pure Cu ingots (purity greater than 99.99%), Cu alloys containing a bulk content of 0.008 wt% Bi or 0.92 wt% Sb were cast in a vacuum induction furnace. After casting, the ingots underwent a thermomechanical processing sequence involving rotary swaging and intermediate annealing treatments. Detailed descriptions of this processing procedure have been published previously by some of the present authors [24, 25]. After swaging, final annealing treatments were performed to establish fully recrystallized homogeneous microstructures with comparable grain sizes and near-equilibrium segregation of Bi and Sb at the grain boundaries. The final grain sizes are given in Table 2 along with the chemical compositions and annealing conditions. In this study, annealing at 823 K for 48 h will be referred to as high temperature (HT) whereas annealing at 723 K for 288 h will be referred to as low temperature (LT) annealing treatment. Miniature creep specimens [26] were machined by spark erosion from the swaged and recrystallized rods and creep tested until rupture in an inert gas atmosphere at temperatures of 773, 823, and 873 K under stresses of 10, 15, and 20 MPa. The inert gas atmosphere miniature creep testing technique has been described previously by Peter et al. [27].

The microstructural assessment procedure is illustrated in Fig. 3 for a Cu-Sb sample tested until fracture at a stress

Table 2 The chemical compositions, final annealing conditions, and grain sizes of the six model materials along with their short names used in the text

Material state	Cu HT	Cu LT	Cu-Bi HT	Cu-Bi LT	Cu-Sb HT	Cu-Sb LT
Composition	Pure Cu > 99.99%		Cu-0.008 wt% Bi		Cu-0.92 wt% Sb	
Annealing treatment	48 h, 823 K	288 h, 723 K	48 h, 823 K	288 h, 723 K	48 h, 823 K	288 h, 723 K
Grain size (μm)	277	76	260	177	316	288

of 20 MPa and a temperature of 823 K. The geometry of the miniature creep specimen is depicted on the left-hand side of Fig. 3a. After rupture, the specimens were cut in half along their longitudinal axis. Metallographic cross-sections were prepared from the inner surfaces by standard methods, and subsequently lightly etched in a solution of 100 mL deionized water and 5 g iron(III) chloride to make the grain boundaries visible in the light microscope such that they may be inspected for intergranular creep damage. Montages of optical micrographs (OM) with a width of 1.2 mm and several mm in length (depending on where fracture took place) were obtained from the center region of the etched cross-sections (dashed rectangle on the miniature creep specimen in Fig. 3a) and compared to EBSD scans of the same areas. An exemplary grain map obtained by EBSD and the corresponding montage from OM are shown to the right of the miniature creep specimen geometry in Fig. 3a. CSL boundaries with $3 \leq \Sigma \leq 29$ were identified from the EBSD data using the B criterion [13]. For every CSL boundary, the actual angular deviation from the ideal CSL misorientation relationship, $\Delta\Theta$, was calculated from the EBSD data following the geometrical technique described by Déchamps et al. [28]. Every identified boundary was then checked for the presence of intergranular damage. A boundary was considered to be damaged when at least one cavity was visible on its trace. Such a scenario is illustrated by the optical micrograph in Fig. 3b where CSL boundaries (identified by the B criterion) are labeled according to their Σ value and non-CSL boundaries are labeled R (for random). It can be seen that the Σ15 boundary in Fig. 3b is cavitated while all Σ3 boundaries are devoid of cavitation. Once such an analysis had been performed, it was easy to apply the more restrictive CSL criteria to the same dataset (see Table 1) because they merely identify a subset of the CSL boundaries that had been found using the B criterion for CSL classification. Further details on the mechanical testing and the microstructural investigation procedures can be found in [22, 23].

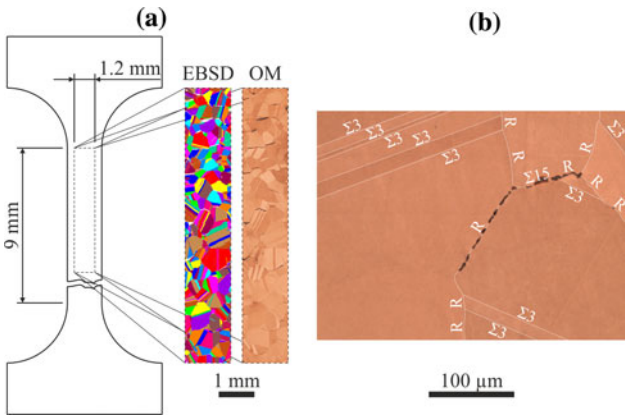

Fig. 3 Illustration of the procedure used for the assessment of the susceptibility of CSL boundaries for intergranular creep damage. **a** EBSD maps and OM were obtained from inner cross-sections of miniature creep specimens (*left-hand side*) tested until rupture. **b** CSL boundaries were identified from the EBSD data and checked for intergranular creep damage

Simulations were performed to determine how the experimental observations compared to the misorientations that result between pairs of randomly orientated grains. For the simulations, random orientation data was generated in the form of unit quaternions using a computer program [29] following the method suggested by Ulrich [30] for sampling the Bingham distribution on the unit sphere. It should be noted that for quaternions the Bingham distribution is essentially the same as the von Mises-Fisher matrix distribution [31–33], which may be better known to materials scientists familiar with the EBSD literature [34]. In all cases for the simulations, a null clustering parameter was used such that the generated data was distributed uniformly over the unit sphere. The misorientation axis and angle were taken between the pairs of randomly generated orientations. Over 6×10^7 randomly generated misorientations were analyzed so that the probability of obtaining coincidental matches to CSL orientation relationships could be compared to the experimental results. The simulation results were in good agreement with Morawiec et al. [35]. In both the analyses of the experimental and simulation results, when a boundary simultaneously matched multiple Σ values (which happens relatively frequently under the B criterion [35, 36]), the lowest matching Σ value was used.

Results

Table 3 provides some quantitative background information concerning the grain boundary analyses conducted in this study. It features the total numbers of grain boundaries

Table 3 Total numbers of grain boundaries (damaged and undamaged) investigated and the raw counts of CSL boundaries with $3 \leq \Sigma \leq 29$ for all six material states identified using the Brandon criterion (B) and the Ishida-McLean criterion (I-M)

Material state	Cu HT		Cu LT		Cu-Bi HT		Cu-Bi LT		Cu-Sb HT		Cu-Sb LT	
Total no of GBs investigated	3755		2583		7200		6285		4111		5137	
Criterion	B	I-M	B	I-M	B	I-M	B	I-M	B	I-M	B	I-M
Σ3	1357	1150	828	622	2271	1765	2003	1715	1213	856	1597	1276
Σ5	3	–	5	–	36	–	49	–	32	–	34	5
Σ7	26	–	12	–	44	–	29	–	26	–	24	1
Σ9	228	37	160	14	301	27	261	39	73	10	96	12
Σ11	21	–	11	–	42	1	24	–	34	–	28	–
Σ13a	7	–	4	–	16	–	11	–	8	–	4	–
Σ13b	15	–	7	–	20	–	16	–	8	–	8	–
Σ15	4	–	4	–	33	1	29	–	20	–	25	–
Σ17a	1	–	1	–	7	–	2	–	1	–	6	–
Σ17b	10	–	4	–	26	–	18	–	19	–	11	–
Σ19a	20	–	7	–	19	–	20	–	3	–	9	–
Σ19b	12	–	7	–	14	–	9	–	7	–	8	–
Σ21a	11	–	3	–	9	–	10	–	6	–	7	1
Σ21b	9	–	4	–	28	–	14	–	11	–	25	–
Σ23	9	–	7	–	16	–	7	–	8	–	15	–
Σ25a	1	–	3	–	4	–	6	–	4	–	3	–
Σ25b	9	–	13	–	20	–	25	–	13	–	23	–
Σ27a	21	–	16	–	28	–	20	–	9	–	12	–
Σ27b	25	1	14	–	26	–	38	–	10	–	7	–
Σ29a	1	–	1	–	–	–	1	–	–	–	1	–
Σ29b	7	–	5	–	18	–	9	–	11	–	13	–
Total no of CSL boundaries	1797	1188	1116	636	2978	1794	2601	1754	1516	866	1956	1295
Fraction of GB having CSL character	0.48	0.32	0.43	0.25	0.41	0.25	0.41	0.28	0.37	0.21	0.38	0.25

investigated for each material state as well as the numbers of different CSL boundary types found when either the B or the I-M criterion was employed for CSL classification. The last row contains the total number of CSL boundaries, which is simply a summation of the all CSL types between Σ3 and Σ29. The data in Table 3 should help the reader to get some sense of the statistical significance of the results which are presented over the course of this article. As a first result from Table 3, it should be noted that CSL boundaries make up about 37–48% of all grain boundaries when the liberal B criterion is used. As one would expect, this number decreases significantly when a more restrictive criterion such as I-M is used. It is, however, striking that CSL boundaries of all Σ values up to 29 can be found using the B criterion while CSL boundaries are almost exclusively composed of the Σ3 and Σ9 types when the I-M criterion is employed for classification. Only *ten out of 7533* considered CSL boundaries make an exception to this remarkable trend.

Figure 4 shows the fractions of CSL boundaries (both damaged and undamaged) with respect to the total number of investigated grain boundaries in each material state, after breaking them down according to their Σ value for the B and I-M classification criteria. The values obtained using these two criteria are given as black and hashed columns, respectively. The gray line represents the expected number fractions obtained by the simulations (under the B criterion), which assumed a random orientation distribution (i.e., a textureless material). For illustration purposes, CSL boundaries of Σ3 and Σ9 types are omitted from the analysis since they are represented in disproportionately high fractions in the materials. Although, the numbers of CSL boundaries with $\Sigma \neq (3,9)$ are relatively low (see Table 3), certain trends can be seen with respect to the simulation results. The best fit between experimental and theoretical data is obtained for Cu-Sb while pure Cu exhibits the strongest deviations. Although not present in great numbers, the percentages of CSL boundaries with

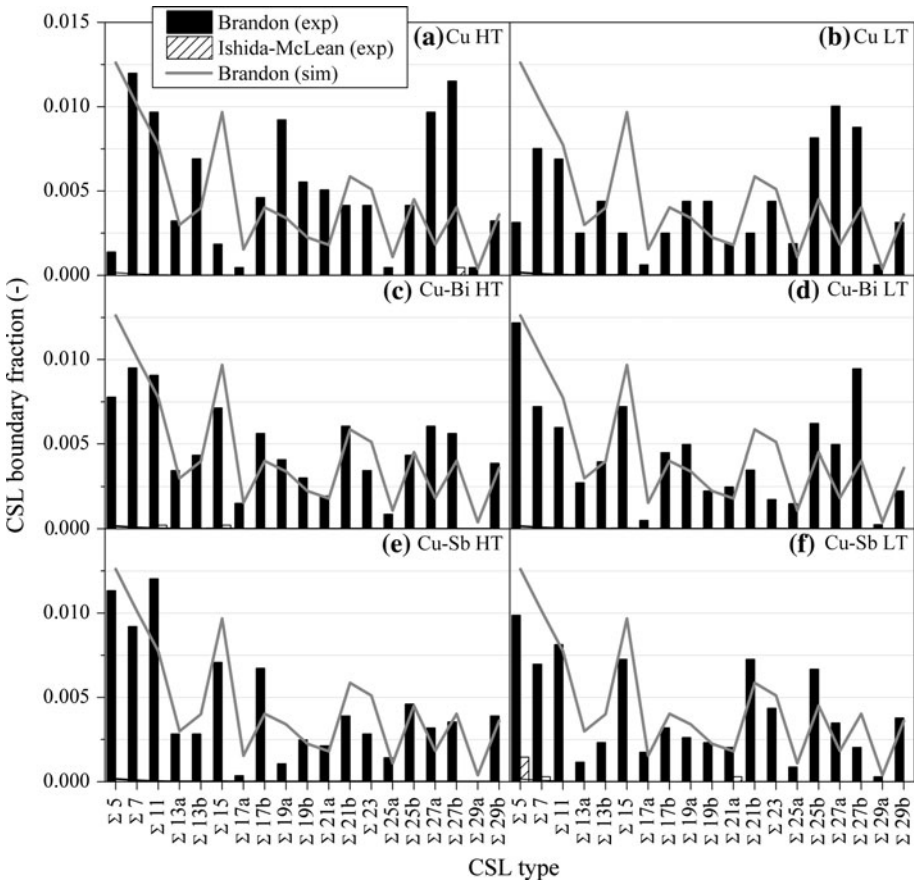

Fig. 4 Fractions of boundaries exhibiting CSL character according to the Brandon criterion (*full columns*) and the Ishida-McLean criterion (*hashed columns*) for the six model material states: **a** Cu HT; **b** Cu LT; **c** Cu-Bi HT; **d** Cu-Bi LT; **e** Cu-Sb HT; and **f** Cu-Sb LT. Fractions expected from a textureless material, as calculated by the simulations, are shown as a *gray line*

$\Sigma = 5$ or 15 appear to be systematically higher for Cu-Sb and Cu-Bi as compared to pure Cu; thus, they create a better match with the simulation results (gray line). On the other hand, boundaries with $\Sigma = 27$ can be most frequently observed in pure Cu. As was indicated already by the numbers in Table 3, almost no CSL boundaries with $\Sigma \neq (3,9)$ can be observed when the I-M criterion is used for classification.

To explain the dominance of $\Sigma 3$ and $\Sigma 9$ boundaries in the CSL populations of our Cu model materials, the deviations of all boundaries from the ideal CSL orientation relationships were considered. Figure 5 compares the relative distributions of $\Sigma 3$, $\Sigma 9$, and $\Sigma \neq (3,9)$ CSL boundaries as a function of the deviation from the ideal CSL orientation relationships under the B criterion. To compare CSL boundaries with different Σ values, the deviation for each boundary was normalized by dividing the absolute angular deviation $\Delta\Theta$ by the maximum allowed deviation $\Delta\Theta_{max}$ (which decreases with increasing Σ, as can be seen in Fig. 2). The deviation distributions for $\Sigma 3$ fit well to a log-normal distribution between the 10th and 90th percentiles, with peaks located between 10 and 20% of the maximum allowed deviation. A similar observation can be made in the case of the $\Sigma 9$ boundaries, with peaks being shifted to higher relative deviations. No such distribution can be fitted for boundaries with $\Sigma \neq (3,9)$ because the CSL fractions increase toward higher deviations. The wedge-shaped areas shaded gray in Fig. 5 again represent simulation results assuming a textureless material. It was found phenomenologically that the following functional dependence exists between the relative CSL boundary fraction f_{CSL} and the deviation from the ideal CSL orientation relationship where n_{bins} is the number of bins used for the distributions:

$$f_{csl} = \frac{3}{n_{bins}} \left(\frac{\Delta\Theta}{\Delta\Theta_{max}} \right)^2 \quad (2)$$

where f_{CSL} sums to unity.

Figure 6 lists number fractions of damaged (cavitated) CSL boundaries with $3 \leq \Sigma \leq 29$ (open columns) which were classified using the four criteria given in Table 1 for each of the six material states after creep exposure. It is evident that the number fractions of damaged grain boundaries which may be classified as CSL boundaries decrease when a more restrictive criterion is used (i.e., a smaller maximum deviation is allowed from the ideal CSL orientation relationship). For pure Cu annealed for 48 h at 823 K (Cu HT), this decrease is very low (3.7 to 2.3%) between the least and most restrictive criteria. In contrast, a strong decrease can be seen for Cu-Sb after the same annealing

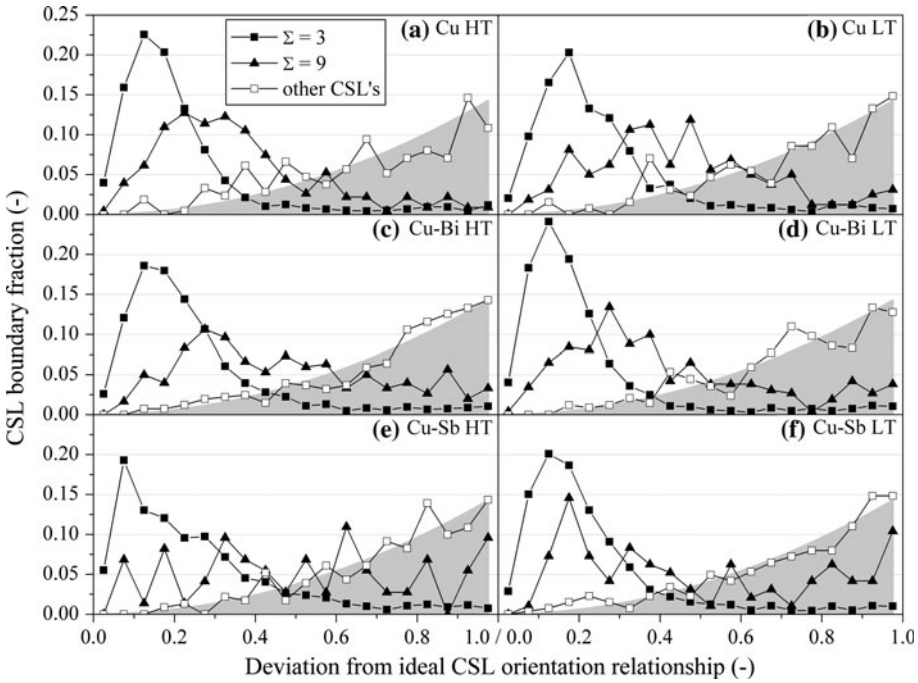

Fig. 5 Distributions of the normalized deviation from the ideal CSL orientation relationship for Σ3 (*filled squares*), Σ9 (*filled triangles*), and Σ ≠ (3,9) (*open squares*) boundaries under the B criterion for the six model material states: **a** Cu HT; **b** Cu LT; **c** Cu-Bi HT; **d** Cu-Bi LT; **e** Cu-Sb HT; and **f** Cu-Sb LT. *Gray shaded region* represents the fractions expected from a textureless material, as calculated by simulations

treatment (7.9% to zero). It was surprising that pure Cu showed the highest fractions of damaged CSL boundaries when the most restrictive classification criterion was used since additions of Bi and Sb adversely affect the resistance to creep cavity nucleation in Cu [22, 23]. Closer inspection revealed that the Cu samples frequently exhibited creep cavities associated with the ends of twin boundaries—a situation that was flagged as a damaged boundary in our initial analysis procedure. An example of such a feature is given in Fig. 7, which shows an EBSD map in which a twin extends between two cavities (black). The twin ends abruptly in the paper plane when it reaches the cavities. Such features are likely inconsequential to the mechanical behavior when the failure mode is intergranular (such as under the presently considered conditions), since they do not appear to be connected to any non-twin boundaries in the grain boundary network. Unfortunately, it was generally impossible to determine if the cavities nucleated on these boundaries (or on their incoherent segments that were not parallel to a {111} plane), if they played an active role in creating the twin, or if they were simply found on migrating twin boundary segments when the creep exposure was interrupted. These features were never observed in Cu-Bi and Cu-Sb, where the segregating species appear to more effectively hinder the grain boundary motion. Significant grain growth was sometimes observed for pure Cu under creep conditions and cavities associated with twin boundaries did not exist in the material before creep exposure, so it seems likely that such features could merely be artifacts arising from the high grain boundary mobility in pure Cu compared to the materials containing grain boundary segregation.

The pure Cu results were then re-analyzed for such artifacts and all cavities that were associated only with the termination of Σ3 twins were removed from the analysis. The results after this error correction procedure are given as the solid black columns in Fig. 6, and the expected lower damage fractions are produced due to the elimination of many of the artifacts like the one shown in Fig. 7. This should represent a fairly conservative estimate for the

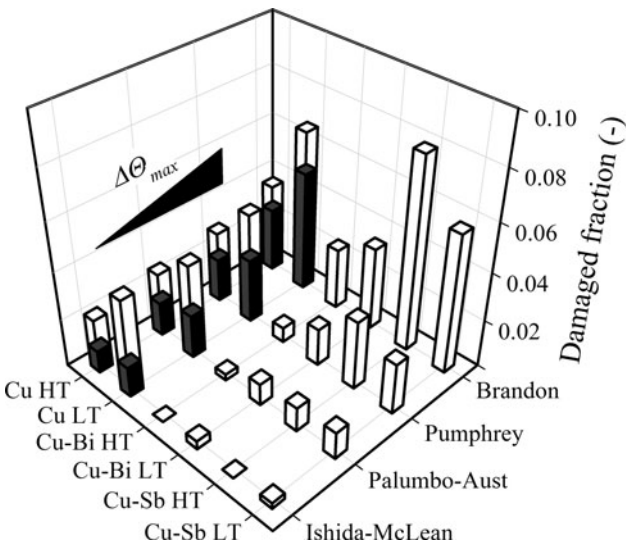

Fig. 6 Fractions of damaged CSL boundaries under the different maximum deviation criteria for the six model material states. *Filled regions* represent the modified values after adjustment for artifacts associated with twin boundaries terminating at cavities

number of artifacts, since only clear examples of twins terminating in isolated cavities were removed, while ambiguous cases were allowed to remain in the analysis.

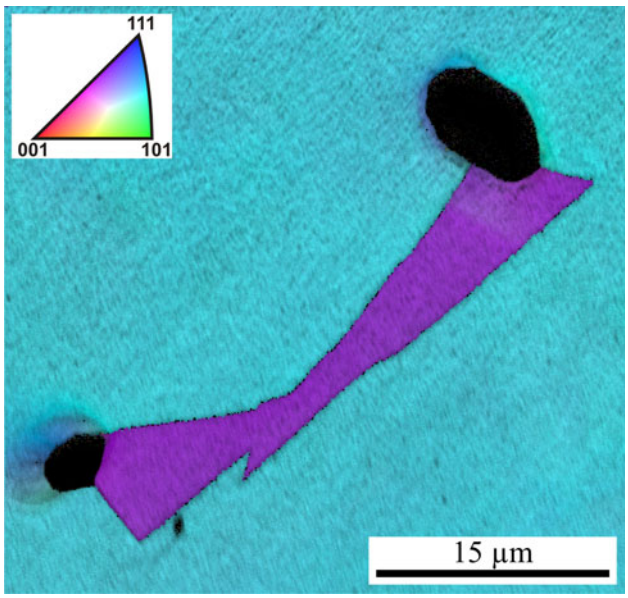

Fig. 7 Twin extending between two cavities in Cu crept at 15 MPa and 823 K

Figure 8 shows scatter plots of all of the CSL boundaries identified in each material versus their relative deviation from the ideal CSL relationship, with the maximum deviation defined by the B criterion. Lines corresponding to the other criteria are shown for comparison; points falling beneath these lines would qualify as CSL boundaries under those criteria. Damaged boundaries are shown as circles while undamaged boundaries are shown as crosses. The results corresponding to the HT specimens are given in the left column of subfigures, and those for the LT specimens are given in the right column. The rows of subfigures correspond, from top to bottom, to the Cu, Cu-Bi, and Cu-Sb materials. Only one data point is covered up by the legend, an undamaged Σ17b boundary with $\Delta\Theta/\Delta\Theta_{max} = 0.39$. In all of the samples, the damage probability generally appears to increase with increasing deviation from the ideal CSL relationship for $\Sigma \neq (3,9)$, and the vast majority of the damaged boundaries fall in the deviation range between the B and Pumphreys criteria. The I-M criterion is so restrictive that it eliminates most of the $\Sigma = 9$ boundaries (both damaged and undamaged), which appear in much higher proportion than would be expected from a random distribution.

When the damaged CSL boundaries from Figs. 6 and 8 are categorized according to their respective Σ values,

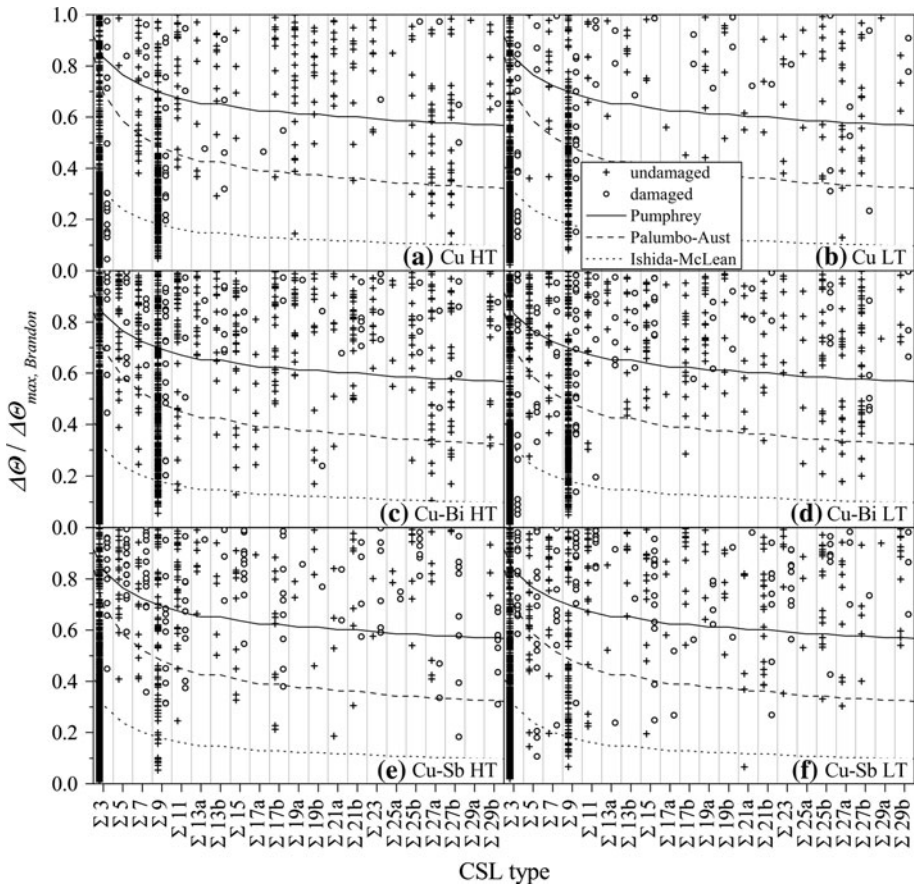

Fig. 8 Normalized deviations from the ideal CSL orientation relationships for damaged and undamaged CSL boundaries, under the B criterion. Most damaged CSL boundaries fall between Brandon's and Pumphrey's criteria. Little difference in cavitation probability is observed between the non-Σ(3,9) boundaries. The I-M criterion is so restrictive that it eliminates most of the Σ9 boundaries (both damaged and undamaged)

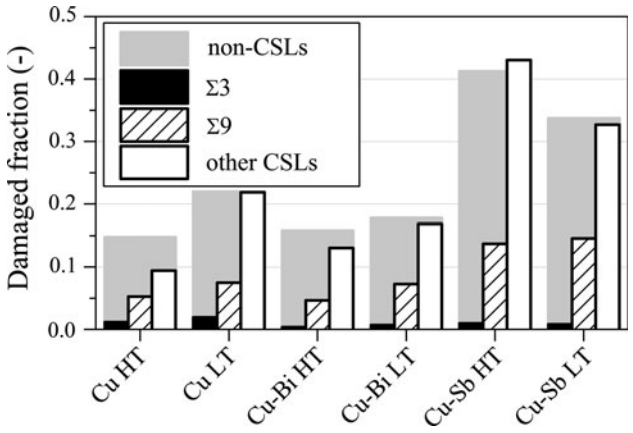

Fig. 9 Damaged fractions of Σ3 (black), Σ9 (*hashed*), and $\Sigma \neq (3,9)$ (*white*), as compared to the non-CSL boundaries (*gray*). The damaged fraction of Σ3 boundaries is not affected by the presence of segregating species, whereas CSL boundaries with $\Sigma > 3$ are observed to be affected by the presence of Sb. Relatively little difference is observed between the damaged fractions of non-CSL boundaries and $\Sigma \neq (3,9)$ boundaries

another trend can be observed. Figure 9 shows the fractions of damaged CSL boundaries with $\Sigma = 3$ (black columns), $\Sigma = 9$ (hashed columns), and other CSL boundaries (white columns) using the B criterion for CSL classification. Non-CSL boundaries are shown in gray for comparison. For pure Cu, the clear cases of erroneously identified damaged twin boundaries were removed as previously described (the black columns in Fig. 6). The fractions of damaged CSL boundaries were obtained individually for each Σ type by dividing the number of damaged boundaries by the total number of boundaries of that respective type found in each material state. For simplicity, the results for $\Sigma \neq (3,9)$ are combined (in the white columns), as they were in Fig. 5. It can be seen that Σ3 boundaries are very damage resistant, with damaged fractions of less than two percent; however, CSL boundaries with $\Sigma \neq (3,9)$ exhibit damaged fractions on the order of the non-CSL damaged grain boundary fractions in almost all cases. In all of the materials studied, Σ9 boundaries were observed to be more likely to cavitate than Σ3 boundaries but less likely than $\Sigma \neq (3,9)$ and non-CSL boundaries.

Discussion

CSL boundaries and creep cavitation damage

While it is clear from Fig. 6 that Sb dramatically worsens the creep cavitation resistance, the weakening effect of Bi on the interfaces is not immediately apparent because the damaged CSL fractions are similar in the cases of Cu and Cu-Bi. To put these numbers into perspective, it must be noted that the rupture times of Cu-Bi were at best 30% of the rupture times of pure Cu under identical testing conditions [22, 23]. Therefore, the damage in Cu-Bi is indeed significant because similar damaged fractions to Cu are exhibited at much shorter creep exposures. Furthermore, the mean cavity size in Cu-Bi was observed to be smaller than that of pure Cu [22, 23], so it also remains possible that the damaged grain boundary fraction in Cu-Bi is actually higher at rupture than in pure Cu but the small cavities did not yet have time to grow large enough to be detected by our microscopy procedure.

The differences in the magnitudes of damaged CSL fractions between the different model materials have to be interpreted in the context of segregation-induced changes in the interfacial chemistry of boundaries with $\Sigma > 3$. In fact, segregation of Bi to Σ5 [37] and Σ9 [38] CSL boundaries has been reported in the literature while Σ3 twin boundaries have been observed to be devoid of segregation [39, 40]. In experiments on Cu-Sb bicrystals containing symmetric tilt boundaries, elevated concentrations of Sb were reported to be present on all CSL boundaries investigated except for low-angle grain boundaries (Σ1) and twin boundaries (Σ3) [41, 42]. Taking into account the significantly lower rupture times observed in the Cu-Bi materials [22, 23], this study shows that CSL boundaries with $\Sigma > 3$ containing detrimental segregants are very likely to exhibit worse properties than they would in a pure material. Thus, these observations appear to be in line with previous studies showing that only Σ3 boundaries have any special resistance to segregation [38–40].

In grain boundary migration experiments on near-Σ5 boundaries, Demianczuk and Aust observed a reduction in mobility as the deviation from the ideal misorientation relationship increased in both pure Al and Al doped with Cu [43]. Under the CSL theory, it would seem reasonable to assume that segregation would be stronger for boundaries deviating from the ideal CSL orientation relationship since an increase in the number of solute atoms may reduce local stresses arising from the strain fields of the grain boundary dislocations associated with the losses in the theoretical structural periodicity of the grain boundary [44, 45]. This relationship between grain boundary character and predilection toward segregation has to be kept in mind when one tries to establish predictive relationships between the fractions of CSL boundaries and properties such as creep cavitation resistance.

Lim and Raj considered both boundary cavitation and deviation from ideal CSL relationships in their study of low-cycle fatigue damage in Ni [46]. They concluded that a dependency exists between the magnitude of the CSL Σ value, the deviation from the ideal orientation relationship, and the cavitation susceptibility, such that higher Σs and higher deviations produce greater likelihoods of cavitation.

Relatively few of their observations were of low Σ boundaries that were not $\Sigma 3^n$ boundaries (i.e., related to twinning), and their conclusions were based on only a small fraction of the number of observations made in this study. Our results in Fig. 8 are clearly in good agreement with their observations. A lower likelihood of cavitation is generally observed for low deviations except for the case of the Σ3 boundaries in pure Cu, for which artifacts such as those in Fig. 7 exist. This lower likelihood observed for low deviations corresponds closely with the probability of any random orientation falling within the CSL criterion, as shown in Fig. 5. Our results do not, however, appear to indicate that the fraction of damaged boundaries increases with increasing Σ, contrary to the conclusions of Lim and Raj [46]. Rather, little difference in cavitation probability is observed between CSL boundaries that are not Σ(3,9). There is a clear change in cavitation probability that occurs with the addition of segregants, as can be seen by comparisons between subfigures in Fig. 8, but the increase in cavitation probability occurs rather uniformly across all CSL Σ values, with the obvious exception of Σ3, and to a lesser extent, Σ9. The absolute differences in the percentage of damaged boundaries observed between pure Cu and in particular Cu-Sb (Fig. 9) are thought to be related to segregation-induced effects.

In regard to the relatively high values of damaged Σ3 boundaries shown for pure Cu in Figs. 8 and 9, it must be noted that when the artifacts (Fig. 7) were ambiguous, they were not removed in the analyses shown in this article. Due to this conservative approach, it remains likely that a substantial number of the remaining damaged Σ3 boundaries identified in the Cu specimens may also be artifacts and not truly creep damage. Looking at the results obtained for Cu-Bi and Cu-Sb, one would expect the fraction of damaged Σ3 boundaries in Cu to approach zero when the I-M criterion is used, due to the very restrictive maximum deviation values of this criterion (see Fig. 8). If it is assumed that the I-M values represent a sort of estimate for the erroneously identified damaged Σ3 boundaries in the counting statistics, then subtracting these values from the B values could serve as an alternative option for estimating the number of such artifacts. Indeed, when this is done, the damaged fractions of Σ3 boundaries in the pure Cu materials in this study are more on par with the values obtained for the Cu-Bi and Cu-Sb results.

CSL criteria and "specialness"

The existence of several competing maximum deviation criteria for CSL boundaries is the result of various authors using differing assumptions concerning local dislocation structure as boundaries deviate from ideal CSL orientation relationships [47]. From an experimental standpoint, the B criterion has sometimes been observed to be too liberal to reliably predict the "specialness" of boundaries [15, 48], and it has been noted that a number of orientations can simultaneously match more than one Σ value [35, 36]. Our results presented in Fig. 6 indeed demonstrate that lower fractions of damaged CSL boundaries are obtained when a more restrictive criterion is used for classification. However, the results presented in Table 3, Fig. 8, and Fig. 9 clearly show that this improved predictability of "specialness" comes primarily from eliminating almost all of the CSL boundaries from the statistics which have Σ values other than three and (to a much lesser extent) nine. As can be seen in Fig. 5, Σ3 boundaries have the most liberal deviation allowance and the maximum allowed angular deviation decreases significantly as Σ increases.

Our study shows that only Σ3 boundaries exhibit exceptional resistance to creep cavitation regardless of boundary chemistry, as shown in Fig. 9. While Σ9 boundaries exhibit an improved resistance to creep cavitation relative to $\Sigma \neq (3,9)$ or non-CSL boundaries, they can become more susceptible to creep cavitation when a segregating species is present (as clearly demonstrated in the case of Cu-Sb). In contrast, Σ3 boundaries were observed to retain their resistance to creep cavitation independent of composition. In our observations, CSL boundaries with $\Sigma \neq (3,9)$ identified under the B criterion did not have a significantly different resistance to creep cavitation from non-CSL boundaries. This is in good agreement with cavitation results from low-cycle fatigue tests on polycrystalline Ni at elevated temperatures [46], and an extension of the findings on intergranular creep damage in the literature where a distinction was normally made only between CSL and general grain boundaries [11, 49–51]. Thus, while this study clearly demonstrates that Σ3 (and to a lesser extent Σ9) boundaries have a remarkable resistance to creep cavitation, our results call into question the "specialness" of the other CSL boundaries. When using the I-M criterion for the identification of CSL boundaries, $\sim 97-99\%$ of all identified CSL boundaries were Σ3 (see Table 3), while only $\sim 80\%$ of the CSL boundaries are Σ3 type when the B criterion is used. Thus, the primary reason for the higher observed percentages of damaged CSL boundaries from using the B criterion comes from the increased fractions of non-Σ3 CSL boundaries, which exhibit no special resistance to creep damage.

It seems clear in light of the results of this study why a distinct advantage has been observed in using a more restrictive criterion than B for identifying boundaries with "special" properties in materials with a high density of Σ3 twin boundaries. Pan et al. [5] made this observation regarding the strictness of the CSL criteria in their investigation of the influence of grain boundary character on intergranular stress corrosion cracking in the Ni-based

alloy X-750. Similar to our Cu-based materials, alloy X-750 is prone to twinning due its low stacking fault energy, and thus exhibits a high percentage of Σ3 boundaries. Pan et al. [5] observed that the percentage of boundaries with $\Sigma = 5$–49 fell from 9.9 to only 2.8% between applying the B criterion [13] and the more restrictive Palumbo-Aust criterion [15], while the fraction of identified Σ3 boundaries remained almost unchanged. Since not a single Σ3 boundary was reported to suffer from cracking, the overall number of damaged CSL boundaries varied according to the maximum deviation allowed by the applied criterion. Our results from Fig. 5, which show the deviations of the ideal CSL orientation relationship, shed some additional light on why this is the case.

An important point in understanding the special role of Σ3 boundaries in terms of their extraordinary resistance to intergranular creep cavitation might come from the fact that their deviation from the ideal CSL orientation relationship is intrinsically low and takes on a different distribution than other CSLs with $\Sigma \neq (3,9)$, as can be seen in Fig. 5. Twin boundaries, which account for the majority of Σ3 boundaries observed, can be expected to have a low deviation due to their nature of formation during annealing. In Cu, and even more in Cu-Sb [22, 23], annealing twins readily form upon recrystallization and grain growth due to the relatively low stacking fault energy. Therefore, their orientation relationship between the twinned and the untwinned lattice is likely to be very close to the ideal twinning orientation relationship (Σ3), giving rise to the approximately log-normal deviation distributions seen in Fig. 5. Furthermore, Randle et al. [52] have shown that annealing of Cu at intermediate temperatures can effectively reorient Σ3 grain boundaries to their lowest energy configuration. While after cold rolling and recrystallization at 1173 K only 15% of the Σ3 boundaries exhibited a symmetric tilt character with {111} boundary planes corresponding to the energetically favorable twinning relationship, they observed that subsequent annealing increased this value to about 68%. Heat treatments at similar temperatures were conducted in this study to create fully recrystallized microstructures with near-equilibrium segregation. The majority of the Σ3 boundaries in our study might therefore be expected to be in a low energy configuration. It seems reasonable to assume that CSL boundaries of other Σ values would also reorient to maximize correspondence between the lattices and minimize deviation from the ideal CSL orientation relationship *if* this would result in a significant minimization of boundary energy (and, by extension, the augmentation of special properties in terms of segregation and cavitation resistance). Grain rotation is also theoretically possible [53], and has been experimentally observed for boundaries with some twist character in the presence of applied stresses [54]. One might then expect that non-Σ(3,9) boundaries that exhibited some degree of specialness in terms of interfacial energy would exist in higher proportions than would be expected from a perfectly random polycrystal, and furthermore should have a deviation from the ideal CSL orientation relationship different from that of random boundaries, as shown in Fig. 5. This was not observable within the statistics of this study, and was not observed in previous studies [55]. While the inclination of the boundary plane was ignored in this study to analyze a significantly larger number of boundaries than is realistically feasible under any currently available 3D technique (such as serial sectioning), and future studies should attempt to account for the boundary plane when possible, these results inevitably lead to the conclusion that there is probably not anything particularly special about the creep cavitation resistance of non-Σ(3,9) boundaries as identified under criteria of the form in Eq. 1. Computational results have also indicated that there may be little correlation between the coincidence of lattice sites and interfacial energy [56], but full experimental verification of this is hindered by the low frequencies of observation of non-Σ(3,9) boundaries [57]. In any case, any specialness that might exist would have little, if any, measurable effect on bulk material properties due to a low probability of occurrence of these boundaries in the material. Therefore, it seems that the best indicator of cavitation resistance of the grain boundaries in the material would simply be the fraction of all boundaries that are Σ3 or Σ9 under a criterion more restrictive than Brandon, but not so restrictive that all of the Σ9 boundaries are excluded (as in the case with the I-M criterion).

It may be possible to explain these observations on Σ9 boundaries (i.e., moderate cavitation resistance, significantly higher than random number fraction), through the fact that they may be formed by a combination of two Σ3 twins [58]. Frary and Schuh [59] derived a new CSL boundary combination rule for triple points, taking into account that the CSL boundaries forming the triple point might deviate from the ideal orientation relationship. Their analysis shows that two intersecting Σ3 boundaries are more likely to form a Σ9 boundary when their individual deviations from the ideal orientation relationship are low. This is in good agreement with our present observations that the deviation distributions for Σ9 in Fig. 5 take on an approximately log-normal distribution, similar to what was observed for Σ3 boundaries but significantly broader. That Σ9 boundaries exhibit a significantly poorer resistance to creep cavitation than Σ3 boundaries suggests that some "special" properties of Σ3 boundaries are retained when two Σ3 boundaries combine to form a Σ9, but the special properties are lost rapidly with compounded deviation from the ideal coincidence across the boundary.

Summary and conclusions

The capabilities of four classification criteria in predicting the degrees of creep cavitation resistance of CSL boundaries have been investigated. The classification criteria (Brandon [13], Pumphrey [14], Palumbo-Aust [15], and Ishida-McLean [16]) are all derived from the Read-Shockley model for low-angle grain boundaries, which states that small lattice misorientations can be accounted for by a set of dislocations. Each classification criterion results in a different value of angular deviation from the ideal CSL orientation relationships, above which it should be assumed that all potential "special" character of the CSL boundary is lost. A large number of grain boundaries in six Cu-based model materials were checked for their grain boundary character and damage state after creep exposure. Boundaries which were identified as having CSL character were then analyzed in detail. From the experimental results, the following conclusions can be drawn:

(1) $\Sigma 3$ boundaries (corresponding to FCC annealing twins) are highly resistant to creep cavitation in all model materials. Boundaries with $\Sigma \neq (3,9)$ do not show special resistance with respect to creep cavitation.
(2) Sb additions in Cu dramatically increase the creep cavitation susceptibility of boundaries with $\Sigma > 3$. This is related to the fact that boundaries with $\Sigma > 3$ show interactions with segregants while $\Sigma 3$ boundaries are generally devoid of segregating impurities.
(3) Boundaries with $\Sigma = 3$ or 9 exhibit a nearly log-normal distribution of angular deviations from the ideal CSL relationship. Boundaries with $\Sigma \neq (3,9)$ exhibit higher average angular deviations from their respective CSL orientation relationships, and the distribution of these deviations approaches the shape that would be expected for a random textureless polycrystal.
(4) The improvement in the capability of predicting "special" behavior that is observed when using one of the more restrictive CSL classification criteria comes primarily from eliminating boundaries with $\Sigma > 3$ from the statistical evaluation, since these boundaries generally do not differ in creep cavitation resistance from random grain boundaries. In polycrystalline FCC materials with low stacking fault energies, non-twin-related CSL boundaries do not seem to be produced in frequencies greater than the random case by a systematic mechanism during processing. Therefore, while it remains possible that some boundaries with Σ values other than 3 or 9 may exhibit extraordinary creep cavitation resistance, they are unlikely to have an important effect on the properties of the material.

Acknowledgements The authors acknowledge financial support by the Deutsche Forschungsgemeinschaft (DFG) through projects EG 101/13-1 and EG 101/13–2. GE acknowledges support through his Max-Planck-Fellow research group at the Max-Planck Institut für Eisenforschung (MPIE), Düsseldorf. FO acknowledges funding through the Advanced Study Group for Input Data and Validation of the Interdisciplinary Centre for Advanced Materials Simulation (ICAMS) at Ruhr-Universität Bochum.

References

1. Koch CC, Ovid'ko IA, Seal S, Veprek S (2007) Structural Nanocrystalline Materials. Cambridge University Press, New York
2. Kaesche H (2003) Corrosion of metals. Springer, Berlin
3. Joseph B, Picat M, Barbier F (1999) Eur Phys J 5:19
4. Riedel H (1987) Fracture at high temperatures. Springer, Berlin
5. Pan Y, Adams BL, Olson T, Panayotou N (1996) Acta Mater 44:4685
6. Takashima M, Wynblatt P, Adams BL (2000) Interface Sci 8:351
7. Field DP, Adams BL (1992) Acta Metall Mater 40:1145
8. Randle V (1996) the role of the coincidence site lattice in grain boundary engineering. The Institute of Metals, London
9. Kronberg ML, Wilson FH (1949) Trans AIME 185:501
10. Watanabe T (1984) Res Mech 11:47
11. Lehockey EM, Palumbo G (1997) Mater Sci Eng 237:168
12. Jones R, Randle V (2010) Mater Sci Eng 527:4275
13. Brandon DG (1966) Acta Mater 14:1479
14. Pumphrey PH (1976) In: Smith DA, Chadwick GA (eds) Grain boundary structure and properties. Academic Press, London, p 139
15. Palumbo G, Aust KT (1990) Acta Metall 38:2343
16. Ishida Y, McLean M (1973) Philos Mag 27:1125
17. Read WT, Shockley W (1950) Phys Rev 78:275
18. Schmelzle R, Muschik T, Gust W, Predel B (1991) Scripta Metall Mater 25:1981
19. Wagner WR, Tan TY, Balluffi RW (1974) Philos Mag 29:895
20. Joshi A, Stein DF (1971) J Inst Met 99:178
21. Inman MC, McLean D, Tipler HR (1963) Proc R Soc London Ser 273:538
22. Otto F (2011) Doctoral Dissertation, Ruhr-Universität Bochum, Bochum
23. Otto F, Viswanathan GB, Payton EJ, Frenzel J, Eggeler G, manuscript in preparation
24. Otto F, Frenzel J, Eggeler G (2011) Int J Mater Res 102:363
25. Otto F, Frenzel J, Eggeler G (2011) J Alloys Compd 509:4073
26. Kolbe M, Murken J, Pistolek D, Eggeler G, Klam HJ (1999) Mat wiss Werkst 30:465
27. Peter D, Otto F, Depka T, Nörtershäuser P, Eggeler G (2011) Mat wiss Werkst 42:493
28. Déchamps M, Baribier F, Marrouche A (1987) Acta Metall 35:101
29. Jung S, Foskey M, Marron JS (2011) Ann Appl Stat 5:578
30. Ulrich G (1984) Appl Stat 33:158
31. Prentice MJ (1986) J R Statist Soc B 48:214
32. Wood ATA (1987) Commun Statist Simula 16:885
33. Wood ATA (1994) Commun Statist Simula 23:157
34. Krieger Lassen NC, Juul Jensen D (1994) Acta Cryst A 50:741
35. Morawiec A, Szpunar JA, Hinz DC (1993) Acta Metall Mater 41:2825
36. Morawiec A (2010) Acta Cryst A 66:717
37. Duscher G, Chisholm MF, Alber U, Rühle M (2004) Nat Mater 3:621
38. Keast VJ, Williams DB (1999) Acta Mater 15:3999
39. Michael JR, Williams DB (1984) Metall Trans A 15:99

40. Alber U, Müllejans H, Rühle M (1999) Acta Mater 47:4047
41. Monzen R, Matsuda O, Miura H (2002) Z Metallkd 93:840
42. Monzen R, Kuze T, Matsuda O, Miura H (2003) Metall Mater Trans A 34:773
43. Demianczuk DW, Aust KT (1975) Acta Metall 23:1149
44. Gleiter H (1970) Acta Metall 18:117
45. Roy A, Erb U, Gleiter H (1982) Acta Metall 30:1847
46. Lim LC, Raj R (1984) Acta Metall 32:1183
47. King AH, Shekhar S (2006) J Mater Sci 41:7675. doi:10.1007/s10853-006-0665-8
48. Palumbo G, Aust KT, Lehockey EM, Erb U, Lin P (1998) Scr Mater 35:1685
49. Don J, Majumdar S (1986) Acta Metall 34:961
50. Boehlert CJ, Longanbach SC (2008) J Mater Res 23:500
51. Lillo T, Cole J, Frary M, Schlegel S (2009) Metall Mater Trans A 40:2803
52. Randle V, Davies P, Hulm B (1999) Philos Mag 79:305
53. Cahn JW, Taylor JE (2004) Acta Mater 52:4887
54. Gorkaya T, Molodov KD, Molodov DA, Gottstein G (2011) Acta Mater 59:5674
55. Thomson CB, Randle V (1997) Acta Mater 45:4909
56. Olmsted DL, Foiles SM, Holm EA (2009) Acta Mater 57:3694
57. Rohrer GS, Holm EA, Rollett AD, Foiles SM, Li J, Olmsted DL (2010) Acta Mater 58:5063
58. Randle V (2004) Acta Mater 52:4067
59. Frary M, Schuh CA (2003) Acta Mater 51:3731